Asian Journal of Chemistry; Vol. 29, No. 8 (2017), 1757-1760

ASIAN JOURNAL OF CHEMISTRY

https://doi.org/10.14233/ajchem.2017.20610

Microwave Assisted Green Synthesis of Gold Nanoparticles Using *Bougainvillea glabra* Leaf Extract

S. VIDHYA* and A. LEEMA ROSE

Department of Chemistry, Holy Cross College (Autonomous), Tiruchirappalli-620 002, India

*Corresponding author: E-mail: vidhyathanjai@gmail.com

Received: 27 February 2017; *Accepted*: 27 April 2017; *Published online*: 12 June 2017; AJC-18437

Bougainvillea glabra has excellent antimicrobial property and it has good glucose tolerance and significantly reduced intestinal glucosidase activity, with regeneration of insulin-producing cells and increase in plasma insulin. A novel technique for biosynthesis of gold nanoparticles (GNPs) using *B. glabra* as a reductant and offers a green route for the synthesis of GNPs. The synthesized GNPs are characterized by UV-visible spectrophotometer, TEM, EDAX, FTIR and XRD. The synthesized GNPs were mostly oval in shape and the average diameter of GNPs was about 25.71 nm. Energy dispersive X-ray (EDAX) spectrometer confirmed the presence of elemental gold signal of gold nanoparticles. The nanoparticles are found to be highly crystalline as evidenced by the peaks in XRD pattern corresponding to Bragg reflections from (1 1 1), (2 0 0), (2 2 0) and (3 1 1) planes of the fcc structure.

Keywords: *Bougainvillea glabra*, Gold nanoparticles.

INTRODUCTION

Plants are important as they are environmentally acceptable, inexpensive, readily available, renewable sources of materials ecologically acceptable and organic in nature. It possesses various therapeutic compounds, which are being exploited since ancient time as a traditional medicine. Plant mediated synthesis of nanoparticles is gaining importance due to its simplicity and ecofriendly. The nanoparticles have a greater surface area per weight than larger particles, which causes them to be more reactive and this property reveals them as drug carrier [1]. *Bougainvillea glabra* has excellent antimicrobial property and it has good glucose tolerance and significantly reduced intestinal glucosidase activity, with regeneration of insulin-producing cells and increase in plasma insulin [2]. In the present work, we synthesized gold nanoparticles using *B. glabra* as a reductant using microwave assisted method and characterized the synthesized GNPS. The preliminary phytochemical analysis shows the presence of tannins, flavonoids, steroids, carbohydrates, poly phenols and glycosides. These active constituents are responsible for the antioxidant property of the *B. glabra* leaf extract.

EXPERIMENTAL

Preparation of leaf extract: About 50 g powder was soaked in a 250 mL of methanol under cold percolation method. At regular intervals of time, the filtered extract was distillated in order to collect the crude extract. The extract was stored in an Amper bottle and refrigerated

Green synthesis of gold nanoparticles: In a pilot experiment the solution of leaf extract and chloroauric acid were mixed together. The reaction mixture was kept aside in a microwave oven. The colour change from yellow to deep ruby-red indicated the formation of GNPs. The GNPs obtained as a pellet was dispersed in deionized water for further studies [3].

UV-visible spectroscopy: UV-visible spectrophotometer is one of the important techniques for analysis of synthesized GNPs. After the synthesis, the pure GNPs were characterized by UV-visible absorption spectrophotometer (SPECORD 200 plus, Analytikjena, Germany). The colour change in reaction mixture (metal ion solution + plant extract) was recorded through visual observation. Synthesized GNPs was confirmed by sampling the absorption maxima was scanned by UV-visible spectrophotometer at the wavelength of 400-800 nm.

HR-TEM analysis: HR-TEM images were obtained by using TEM, PHLIPS, CM200, 200Kv in SAIF MUMBAI. The typical HR-TEM images obtained for GNPs sample under different magnifications.

EDAX spectroscopy: The presence of elemental gold of green GNPs was measured by high resolution field emission electron microscope with EDS, nano manipulation system available in SRM University, Chennai. Dry powder of green

GNPs was loaded on the stub using double sided adhesive conductive carbon tapes and analyzed.

X-ray diffraction (XRD) measurement: Determination of crystallinity, phase purity, lattice properties and identification of GNPs was done by XRD studies using powder diffractometer with Cu-K_α radiation, operating at 40 kV and a current of 40 mA (X-ray Diffractometer, XPERT-PRO, at SRM University, Kattankulathur).

FTIR analysis of gold nanoparticles: The interaction between phyto-components and gold nanoparticles was analyzed by Fourier transform infrared (FTIR) analysis. FTIR spectrum of the powder (KBr) pellet was recorded using Perkin-Elmer 1600 FTIR spectrophotometer with a resolving power of 4 cm^{-1}.

RESULTS AND DISCUSSION

Green synthesis of gold nanoparticles: Gold nanoparticles (GNPs) were prepared by mixing 3.75 mL of *B. glabra* leaf extract with 25 mL of 1 mM chloro auric acid in a 100 mL conical flask. The content of the flask were mixed together and irradiated in a micro oven for 60 s. As shown in the Fig. 1 the colour change from yellow to deep ruby-red indicated the formation of GNPs. A clear colour change from pale-yellow to ruby-red was observed within a minute, indicating *B. glabra* extract mediated transformation of chloro auric acid into colloidal GNPs ($Au^{3+} \rightarrow Au^0$) [4].

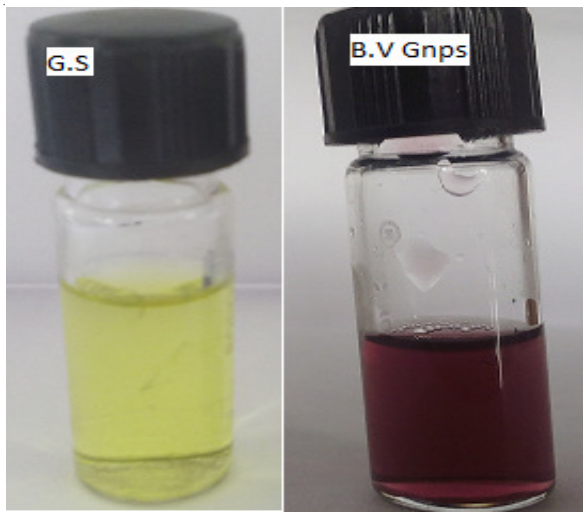

Fig. 1. Visual observation of formation of gold nanoparticles

UV-visible analysis: Colloidal gold nanoparticles are known to display surface plasmon resonance (SPR) characteristics and absorb visible light [5]. The wavelength of absorption maximum is due to the size dependent quantum mechanical phenomena displayed by metal nanoparticles. Therefore, surface plasmon resonance measurements were carried out to confirm the presence of GNPs in the deep ruby-red solution (Fig. 2). Fig. 2 shows a major bands centered about 544 nm. The bands are broad and the intensity increases indicating increase in production of GNPs. A comparison of the SPR band at 544 nm with those reported in the literature confirmed the formation of gold particles in 'nano' dimension [6]. Interestingly, the position of the surface plasmon resonance

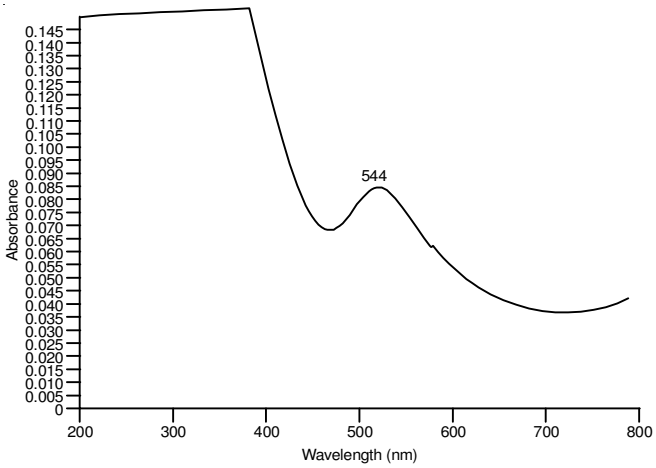

Fig. 2. UV-visible spectrum of gold nanoparticles

band observed at the initial stage of reaction remained almost unaffected even after several hours, implying non-agglomeration of the nanoparticles presumably due to the capping of nanoparticle surface by phytochemical constituents. As to the mechanism of formation of GNPs, the reduction of $Au^{3+} \rightarrow Au^0$ by the phenolic antioxidants and reducing sugars is speculated. Similar reports on the reduction of $Fe^{3+} \rightarrow Fe^{2+}$ by polyphenols with antioxidant activity have been reported in the literature.

TEM analysis: To gain more insight about the size and shape of the synthesized GNPs, high resolution TEM analysis was carried out. Fig. 3a shows the HR-TEM image for GNPs synthesized using *B. glabra* leaf extract. The synthesized GNPs were mostly oval in shape. However, a few large particles with a regular hexagonal shape were also observed. The average diameter of GNPs was about 25.71 nm. The fact that all the nanoparticles are well separated, no clusters or aggregated mass is seen, clearly indicates the stabilization (through capping) of individual nanoparticles by phytochemicals present in the leaf extract. Selected area electron diffraction (SAED) pattern for the GNPs are given in Fig. 3b. The ring like pattern indicates the crystalline structure of GNPs [7].

EDAX analysis: Energy dispersive X-ray (EDAX) spectroscopy is used for the elemental analysis or chemical characterization of a sample. The fundamental principle is that each element has a unique atomic structure allowing unique set of peaks on its X-ray emission spectrum [8]. As the energies of the emitted X-rays are characteristic of the difference in energy between the two shells and of the atomic structure of the emitting element, EDS allows the elemental composition of the specimen to be measured. Analysis of synthesized GNPs through EDAX measurements confirmed the presence of elemental gold (Fig. 4). EDAX spectrum shows the presence of strong elemental gold peak (48.72 wt %), oxygen peak (27.64 wt %), carbon peak (11.88 wt %) and weak sodium peak (1.34 wt %) confirming the presence of gold nanoparticles. Another weak peak corresponding to elemental aluminum could arise from impurities present in the plant extract. The carbon peak might be due to the presence of phytochemicals bound to the surface of GNPs [9].

Powder X-ray diffraction analysis: Powder diffraction data are usually presented as a diffractogram in which the diffracted intensity (I), is shown as a function of the scattering

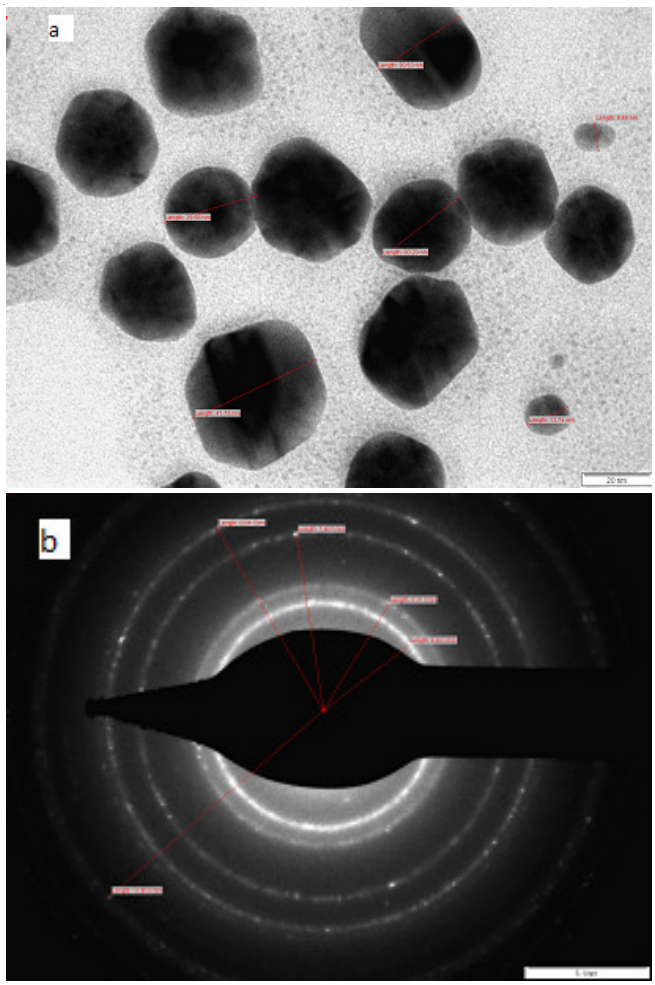

Fig. 3. HR-TEM images of gold nanoparticles

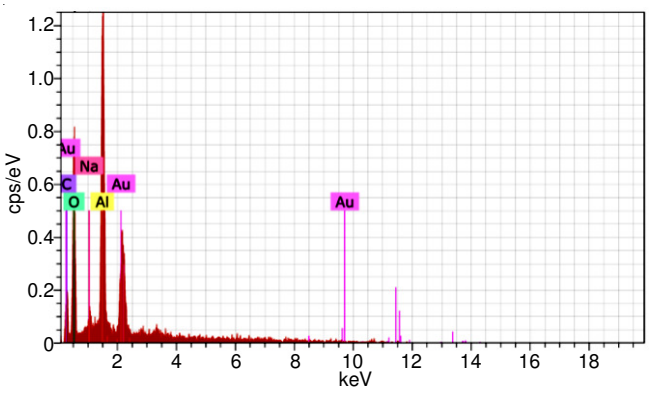

Fig. 4. EDAX of gold nanoparticles

angle 2θ [10]. Powder XRD (copper anode) analysis of synthesized GNPs (Fig. 5) exhibits diffraction peaks corresponding to (111), (200), (220) and (311) phases in the 2θ range of 30º-90º. In the XRD pattern, diffraction peaks at angles of 38.29°, 44.81°, 65.125° and 78.303° could be assigned to face-centered cubic (fcc) metallic gold (111), (200), (220) and (311) facets of gold nanocrystals, respectively [11].

FTIR analysis: Infrared spectra of *B. glabra* leaf extract and the synthesized gold nanoparticles were recorded to gain information about transformation of functional groups present in *B. glabra* leaf extract during the synthesis of gold nanoparticles. The phytochemicals present in the extract would simultaneously act as reducing, stabilizing and capping agents. The FTIR spectrum (Fig. 7) clearly illustrates the biofabrication of gold nanopaticles mediated by the extract.

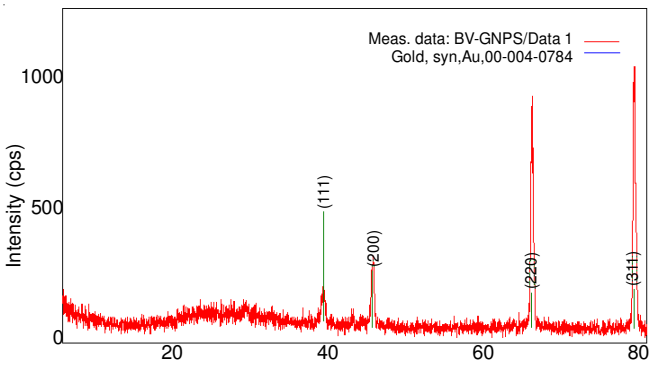

Fig. 5. XRD pattern of gold nanoparticles

The FTIR spectrum of *B. glabra* leaf extract shows a broad peak at 3436 cm^{-1} (Fig. 6) assigned to phenolic –OH which is shifted to 3332.09 cm^{-1} (Fig. 7) due to intermolecular hydrogen bonding [12]. The band at 1631.55 cm^{-1} assigned to carbonyl group (C=O) is shifted to 1636.36 cm^{-1}. Similarly, the peak at

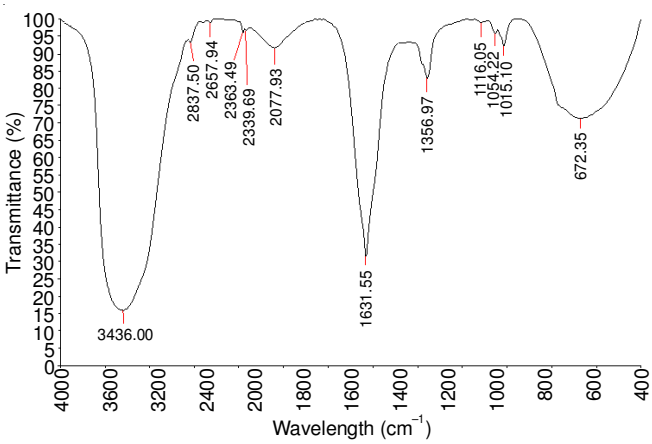

Fig. 6. FTIR spectrum of *B. glabra*

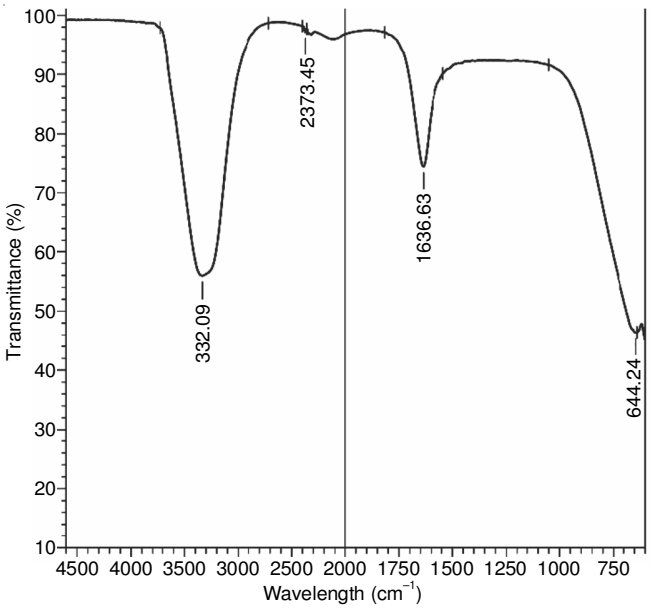

Fig. 7. FTIR spectrum of gold nanoparticles

672.35 cm^{-1} assigned to aromatic ring is also shifted to 644.24 cm^{-1}. FTIR spectra of the extract and the synthesized GNPs revealed that GNPs might be surrounded by molecules like polyphenols, reducing sugars and flavonoids, which are commonly found in plant extracts [13]. These chemical constituents present in the leaf extract are capable of converting chloro auric acid to gold nanoparticles due to their capping and reducing capacities. From these observations it is clear that the phytochemicals present in *B. glabra* leaf extract are responsible for reduction and stabilization by capping of GNPs.

Conclusion

Green synthesis of gold nanoparticles (GNPs) was accomplished using methanolic extract of *B. glabra* leaf. The change in colour from pale yellow to ruby red indicated the reduction of Au^{3+} ions to Au^{0}. Surface plasmon resonance bands of the colloids were centered at 544 nm. The colloid obtained by rapid reduction was found to consist of well-dispersed nearly spherical particles having size around 25.71 nm. Energy dispersive X-ray (EDAX) spectrometer confirmed the presence of elemental gold signal of GNPs. The nanoparticles are found to be highly crystalline as evidenced by the peaks in the XRD pattern corresponding to Bragg reflections from (1 1 1), (2 0 0), (2 2 0) and (3 1 1) planes of the fcc structure. From FTIR, it is clear that the phytochemicals present in *B. glabra* leaf extract are responsible for reduction and stabilization by capping of GNPs.

REFERENCES

1. http://www.pharmainfo.net/book/emerging-trends-nanotechnology-pharmacy-1introduction-nanotechnology/classification.
2. S.A. Fawad, N. Khalid, W. Asghar and H.A.R. Suleria, *Chin. J. Nat. Med.*, **10**, 441 (2012); https://doi.org/10.1016/S1875-5364(12)60085-5.
3. R.K. Mohanty, S. Thennarasu and A.B. Mandal, *Colloids Surf. B Biointerfaces*, **114**, 138 (2014); https://doi.org/10.1016/j.colsurfb.2013.09.057.
4. D.M. Lingappa, *Bioinorg. Chem. Appl.*, **Article ID 341798** (2013); https://doi.org/10.1155/2013/341798.
5. A. Henglein, *J. Phys. Chem.*, **97**, 5457 (1993); https://doi.org/10.1021/j100123a004.
6. S.S. Shankar, A. Rai, A. Ahmad and M. Sastry, *J. Colloid Interface Sci.*, **275**, 496 (2004); https://doi.org/10.1016/j.jcis.2004.03.003.
7. J.Y. Song and B.S. Kim, *Bioprocess Biosyst. Eng.*, **32**, 79 (2009); https://doi.org/10.1007/s00449-008-0224-6.
8. J. Goldstein, Scanning Electron Microscopy and X-Ray Microanalysis, Springer (2012).
9. D.V. Leff, L. Brandt and J.R. Heath, *Langmuir*, **12**, 4723 (1996); https://doi.org/10.1021/la960445u.
10. D. Philip, *Physica E*, **42**, 1417 (2010); https://doi.org/10.1016/j.physe.2009.11.081.
11. D. Inbakandan, R. Venkatesan and S.A. Khan, *Colloids Surf. B Biointerfaces*, **81**, 634 (2010); https://doi.org/10.1016/j.colsurfb.2010.08.016.
12. J. Mohan, Organic Spectroscopy-Principles and Applications, Narosa Publishing House, Delhi, edn 2 (2004).
13. K. Nakamoto, Infrared and Raman Spectra of Inorganic and Coordination Compounds, John Wiley, New York, edn 3 (1978).